Talanta 134 (2015) 264–270

Contents lists available at ScienceDirect

Talanta

journal homepage: www.elsevier.com/locate/talanta

Paper-based microfluidic sensing device for label-free immunoassay demonstrated by biotin–avidin binding interaction

Kin Fong Lei [a,b,*], Shih-I Yang [a], Shiao-Wen Tsai [c], Hsiao-Ting Hsu [c]

[a] Graduate Institute of Medical Mechatronics, Chang Gung University, Taoyuan, Taiwan
[b] Department of Mechanical Engineering, Chang Gung University, Taoyuan, Taiwan
[c] Graduate Institute of Biochemical and Biomedical Engineering, Chang Gung University, Taoyuan, Taiwan

ARTICLE INFO

Article history:
Received 29 September 2014
Received in revised form
14 November 2014
Accepted 15 November 2014
Available online 24 November 2014

Keywords:
Paper-based microfluidics
Label-free immunoassay
Carbon nanotubes
Portable diagnostics

ABSTRACT

Efficient diagnosis is very important for the prevention and treatment of diseases. Rapid disease screening in ambulatory environment is one of the most pressing needs for disease control. Despite there are many methods to detect the results of immunoassays, quantitative measurement for rapid disease screening is still a great challenge for point-of-care applications. In this study, a fabrication method for depositing carbon nanotube bundles has been successfully developed for realization of functional paper-based microfluidic sensing device. Quantitative detection of label-free immunoassay, i.e., biotin–avidin binding interaction, was demonstrated by direct measurement of the current change of the biosensor after single application of the target analyte. Sensitivity of 0.33 μA/ng mL^{-1} and minimal detectable analyte concentration of 25 ng/mL were achieved. The time necessary for the detection was 500 s which is a large reduction compared with the conventional immunoassay. Such paper-based biosensor has the benefits of portability, fast response, simple operation, and low cost and has the potential for the development of rapid disease screening devices.

1. Introduction

Immunoassay is one of the widely used and standard diagnostic techniques nowadays [1]. This bio-analytical technique is based on the specific interaction between an antibody and its antigen. Hence, antigen of a particular disease can be detected by the known antibody. Conventionally, immunoassay is performed on a microplate and involves a series of washing, mixing, and incubation steps between each application of reagents. The entire process requires operating in a well-equipped laboratory and handling by well-trained personnel. That makes diagnostic service in hospital expensive and time-consuming. However, efficient diagnosis is very important for the prevention and treatment of diseases. The need of rapid disease screening devices for quantitative measurement that can operate in clinics or home has been emphasized recently [2–4]. Rapid disease screening for point-of-care (POC) applications often refers to devices which are portable, have fast response, are simple to operate, and are inexpensive [2]. Such technologies hold great impact on improving global health [3,4].

Microfluidic systems built by silicon, glass, or polymer substrates have been extensively developed for POC applications and a lot of excellent bio-analytical demonstrations have been reported recently [5–7]. Although these systems are much more simplified than conventional analytical instruments, they are still not readily accessible to untrained personnel. There are few commercialized microfluidic POC products in the market [8]. In recent years, paper-based microfluidics, or paperfluidics, has been proposed for a new class of POC diagnostic device because paper is inexpensive, thin, lightweight, and disposable [9]. Paperfluidics is realized by patterning sheets of paper into hydrophilic channels bounded by hydrophobic barriers based on the technologies such as photolithography [10,11], wax printing [12,13], polydimethylsiloxane (PDMS) printing [14], and plasma treatment [15]. The barriers define the dimension, i.e., width and length, of the channels and the thickness of the paper defines height of the channels. Therefore, aqueous solution can be passively transported by wicking through the paper fibers. Based on this development, biological analyses, e.g., glucose detection, on paperfluidics were demonstrated by determining the color intensity of the reacted sites visually [16]. Although the colorimetric detection is straightforward, changes of color intensity are difficult to distinguish for quantitative detection because of the influence of color perceptions of people and environmental illumination. To pursue quantitative analysis, digital devices, such as cell phone camera and photosensor, have been used for image capturing and analysis by computer software [17,18]. Moreover, electrochemical detection was also applied using paperfluidics for quantitative biological

* Correspondence to: 4/F., Engineering Building, Chang Gung University, 259 Wen-Hwa 1st Road, Kwei-Shan, Tao-Yuan, 333 Taiwan, ROC.
Tel: +886 3 2118800x5345; fax: +886 3 2118050.
E-mail address: kflei@mail.cgu.edu.tw (K.F. Lei).

http://dx.doi.org/10.1016/j.talanta.2014.11.031
0039-9140/

assays for detection of glucose, uric acid, and lactate [10,19,20]. Conductive carbon and silver pastes were screen-printed on paper to fabricate the detection electrodes. The aforementioned techniques could achieve an important feature of POC devices, i.e., the result was analyzed from a single application of the sample, but they could only detect an enzymatic reaction. Moreover, many nanoparticles were used for the paper-based immunosensor, such as gold nanoparticles, quantum dots, and graphene [21]. Gold nanoparticles and quantum dots were demonstrated to be used in lateral-flow test-strip devices [22–25]. They worked as a label conjugated to secondary antibody for generating optical or electrochemical signal. In addition, graphene was used as a working electrode for the electrochemical detection of immunoassay [26,27]. In this demonstration, horseradish peroxidase (HRP) was used as a label to generate detectable signal detected by graphene electrode. The above excellent demonstrations still rely on a label to generate detectable signal of immune-reaction. Using a label can generate detectable signal; but, it might induce extra operations and time cost.

In this work, we propose a method to fabricate carbon nanotube (CNT)-based biosensor on paper for implementation of a quantitative label-free immunoassay and demonstration of the detection of a biotin–avidin binding interaction. Result can be directly measured by the current change of the biosensor after single application of a sample. The biotin–avidin binding interaction has high affinity and specificity and a lot of standard reagents utilize this binding interaction for diverse detection schemes [28,29]. Because the biotin–avidin interaction is well known and stable, we used it to develop our paper-based microfluidic sensing device. CNT was used as the biological transducer because the conductivity of CNT is highly related to the protein binding on its sidewall. A number of papers in literature have reported that a functionalized single CNT across a pair of metal nano-electrodes can work as label-free protein biosensor [30–33]. However, the difficulty of processing a single CNT is a hurdle for its practical realization. Therefore, use of CNT bundles across the electrodes has been proposed to realize individual functional device. Temperature sensing and pH monitoring of analytes have been respectively demonstrated using the CNT-deposition techniques of ac electrophoresis [34] and spray method [35]. Here, we have adopted a vacuum filtration method to deposit CNT bundles with well-defined dimension to fabricate the biosensor on paper. This method was originally developed for the fabrication of conductive CNT films for use in light-emitting diode (LED) [36–38]. It reported that the method provides deposition of CNT with homogeneity and controlled thickness [36]. We have re-examined it and successfully fabricated a CNT-based sensor on paper to monitor the pH value of the analyte solutions [39,40]. Based on these developments, we have functionalized the CNTs and fabricated a biosensor on paper for label-free immunoassay. Biotin was immobilized on CNT's sidewall and CNTs conjugated to biotin were then deposited on paper by vacuum filtration method to form the biosensor. Avidin suspended solution was applied to the biosensor and their binding interaction was measured by the current change of the biosensor. The CNT-based biosensor showed a sensitivity of 0.33 μA/ng mL^{-1} and a minimal detectable analyte concentration of 25 ng/mL. Such detection is a label-free method and the result of immunoassay can be quantitatively analyzed from single application of sample, which is suitable for POC applications. By demonstrating label-free biotin–avidin detection, label-free immunoassay of specific disease can be extended by replacing the proven antigen–antibody complex.

2. Materials and methods

2.1. Chemicals and reagents

Commercially available single-wall CNTs were used in this study and purchased from Centron Bio-chemistry Technology Co., Taiwan. Filter paper of 800 nm pore size was utilized and purchased from Whatman, USA. Biotin, avidin, bovine serum albumin (BSA), N-Hydroxysuccinimide (NHS), N-(3-Dimethylaminopropyl)-N'-ethylcarbodiimide hydrochloride (EDC), hydrochloric acid (HCl), and sodium hydroxide (NaOH) were obtained from Sigma, Taiwan. PDMS material (Sylgard®184) was purchased from Dow Corning, USA. Buffer used throughout this study was phosphate-buffered saline (PBS; 0.2 M Na_2HPO_4, 0.2 M NaH_2PO_4, pH 6.7).

2.2. Fabrication of the CNT-based biosensor

The fabrication process of the CNT-based biosensor on paper is illustrated in Fig. 1. The CNTs were functionalized based on the reported protocol [41]. The CNTs were bathed in HCl under sonication for 0.5 h to create acid functionality through carboxyl groups (–COOH) on CNT's sidewall. Acid treated CNTs were washed in deionized water, collected by filtration, and dried. The treated CNTs (0.6 mg) were dispersed in PBS buffer (15.5 mL) under sonication for 2 h. NHS solution (2.3 mL of 50 mg/mL) and EDC solution (1.2 mL of 36 mg/mL) were then added to the dispersion and stirred for 0.5 h. Thereafter, biotin solution (1 mL of 20 mg/mL) was added and the solution was then stirred for 24 h at 4 °C followed by the centrifugation and repeated washing with deionized water. Therefore, biotin functionalized CNT suspended solution was prepared for the deposition process. On the other hand, the filter paper was treated by the blocking process (0.1% BSA in PBS) in order to eliminate the non-specific protein binding. Vacuum filtration process was then conducted using a metal mask covering on the filter paper for defining the geometry of the biosensor. The metal mask contained openings of the patterns of the biosensors. It was designed by computer software and

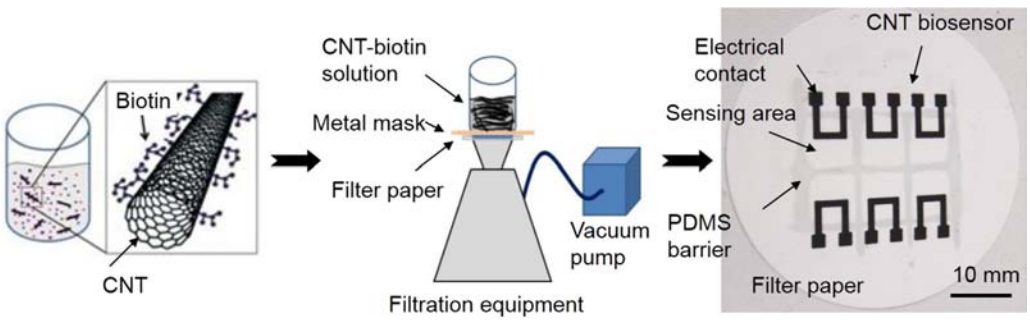

Fig. 1. Fabrication process of the CNT-based biosensor on paper based on vacuum filtration process and photograph of the biosensors with PDMS barrier.

fabricated by the laser micro-machining. The filter paper was the substrate on which the biosensors were built. In the process, the biotin functionalized CNT suspended solution was poured into the container of the vacuum filtration equipment and sucked by the vacuum force. As the solution went through the openings of the metal mask and the pores of filter paper, the CNTs were trapped on the paper surface, forming a homogeneous layer. The filter paper was then removed from the vacuum filtration equipment gently and dried in a dehumidifier at 4 °C, therefore, forming the bundled CNT-based biosensors on the paper. The paper was still flexible and the CNT-based biosensor did not show cracks on the surface under microscopic observation. In this study, six biosensors were fabricated on a single paper, as shown in Fig. 1. In order to define the six sensing areas, a PDMS mixture (PDMS pre-polymer and curing agent in a weight ratio of 10:1) was applied by a pipette on the paper along a pre-designed trajectory and cured for 2 h at 4 °C. PDMS mixture fully penetrated the paper during the curing period and became a fluid-barrier after the curing process. An aqueous solution could only wet the sensing area and not wick through the PDMS barrier. A part of the biosensor inside the sensing area served as a biological transducer and other parts outside the area were responsible for the electrical contacts, two 2×2 mm^2 square blocks, with the measurement equipment. In most of the existing CNT-based sensors, a single CNT or CNT bundles were formed across a pair of metal electrodes for the realization of a functional sensor [30–35]. However, the contact resistance between the CNT and the metal was reported in the order of hundreds of kilo-ohms or mega-ohms [42,43] and this accounted for the variations of the resistance across the sensor [44]. In our work, the milli-scaled electrical contacts should help to improve the consistency of the electrical characteristics of the CNT-based biosensors.

3. Results and discussion

3.1. Physical characterization of the sensor

In the fabrication process, the thickness of the sensors was controlled by the weight of the CNTs used in the vacuum filtration process. Theoretically, more CNTs used in the process can deposit a thicker layer. On our current design of the metal mask, six sensors were batch fabricated on a single paper. Assuming even distribution of the CNT in the solution, the weight of CNTs per sensor was divided by six from the total weight of the CNTs used in the process. That is, if the weight of 0.6 mg is used in the vacuum filtration process, the weight of CNTs per sensor will be 0.1 mg. In order to investigate the controllability of the thickness and electrical characteristic of the sensor, different weights of the CNTs per sensor, i.e., 0.1, 0.2, and 0.3 mg, were respectively used to fabricate the sensors. Note that CNTs were not functionalized by the biotin in this physical characterization study. Fig. 2 reveals the cross-sectional images of the sensors captured by a vertical illuminator (BH2-UMA, Olympus) and the corresponding thicknesses measured by computer software (TSView, Tucsen). The thickness showed a linear proportionality to the weight of CNTs per sensor. It was suggested that this fabrication process provided CNT deposition with well-controlled thickness. To examine the electrical characteristic of the CNT-based sensor, *I–V* measurement was performed using an impedance analyzer (VerseSTAT 4, Princeton Applied Research) under dry and ambient condition. Potentials from −5 to 5 V with 0.01 V step were applied across the sensor. The electrical characteristic of the sensor is shown in Fig. 3. Linear *I–V* response was observed and the conductivity showed a linear proportionality to the weight of CNT per sensor. We believe

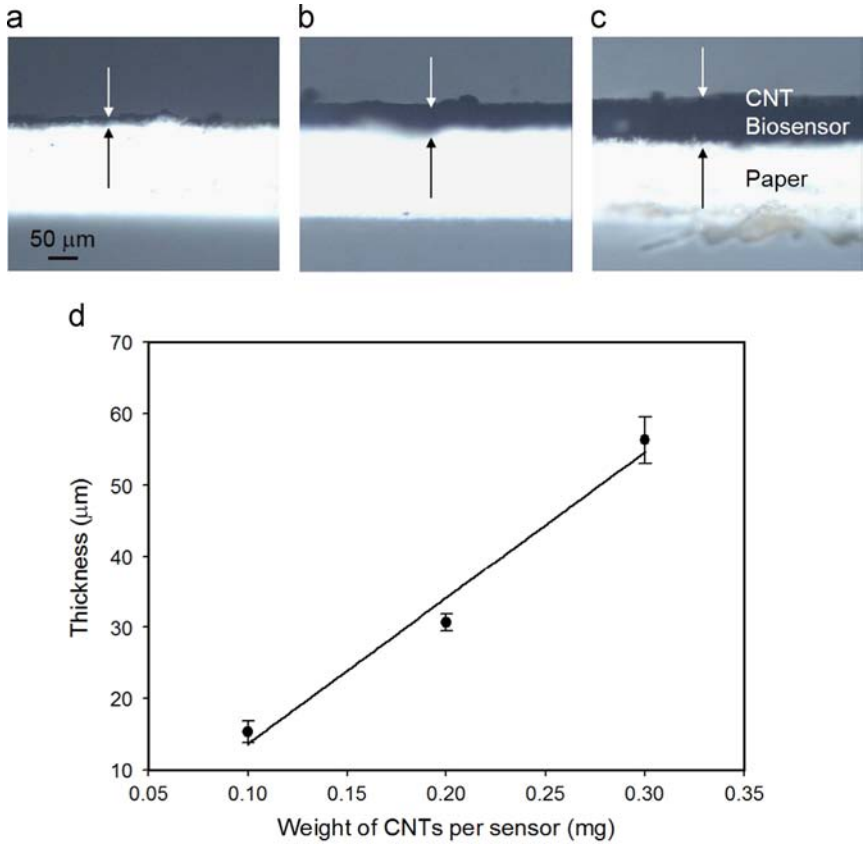

Fig. 2. Investigation of the deposition thickness of the CNT-based biosensor. (a)–(c) The cross-sectional images of the sensors with the weight of CNTs per sensor of (a) 0.1 mg, (b) 0.2 mg, and (c) 0.3 mg. (d) Quantitative correlation between the thickness of sensor and the weight of CNTs per sensor. A linear regression line is shown and error bars represent the standard errors of at least three repeated measurements.

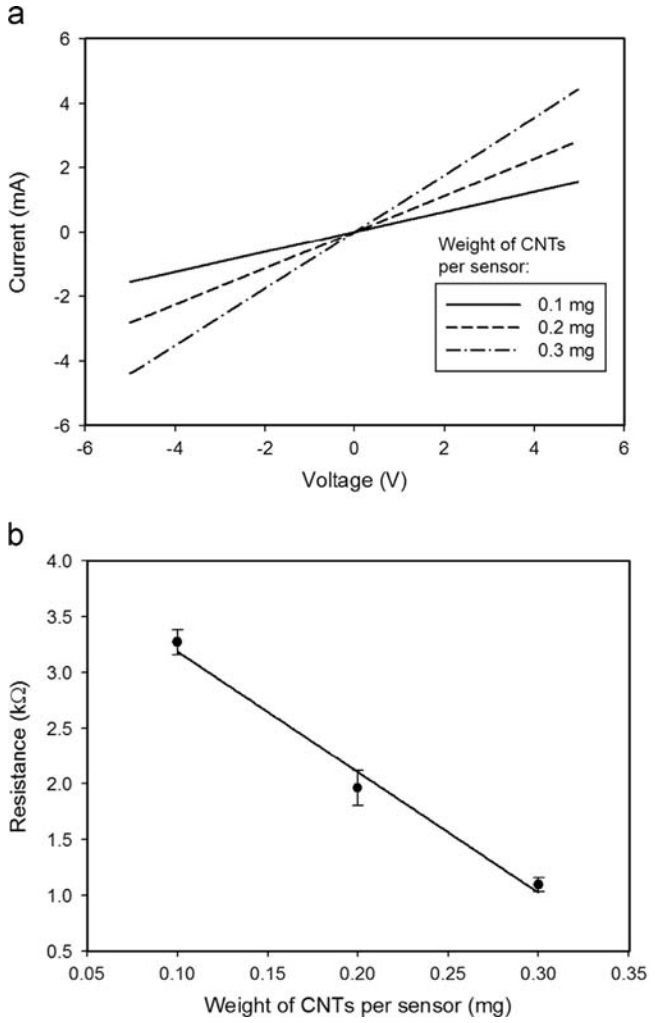

Fig. 3. Electrical characteristics of the CNT-based sensor. (a) *I–V* response of the sensors in different thicknesses. (b) Quantitative correlation between the resistance of sensor and the weight of CNTs per sensor. A linear regression line is shown and error bars represent the standard errors of at least three repeated measurements.

that as the cross-sectional area of the sensor was large, e.g., around $60 \times 1000\ \mu m^2$ in the case of 0.3 mg, the electric power cannot affect the linearity of the *I–V* response in the voltage range from -5 to 5 V. Moreover, it is known that the resistivity of an object is proportional to the cross-sectional area. Since the thickness of the sensor was shown to be corresponding with the weight of CNTs, the resistance across the sensor was also proportional to the weight of CNTs. The results showed that the dimension and the resistance across the sensor can be well controlled by the proposed method. In addition, thickness variations influence the repeatability of the resistance across the sensor. In our study, the variation of the resistance was shown to be limited and hence the uniformity of the deposited CNT over the paper can be guaranteed. This is shown by the limited standard errors plotted in Fig. 3(b). During the vacuum filtration process, the CNTs deposit on the paper and accumulate a certain thickness. If the local region becomes thicker than the surrounding region, the local permeation rate slows down leading to the reduction of the local deposition rate. Therefore, the deposition rate of the surrounding region will increase and homogeneity of the deposition is confirmed. Compared with the previous studies of manipulation of CNT bundles using ac electrophoresis [34] and spray method [35], repeated fabrication of the CNT bundles across the electrodes was difficult. The proposed method provides a simple, efficient, and well-controlled technique to deposit CNT bundles for realizing a functional paper-based microfluidic sensing device.

3.2. Electrical characterization of the sensor in ionic solution

The detection scheme of the proposed CNT-based biosensor is based on the change in conductivity across the sensor and is highly sensitive to the ionic strength of the analyte solution. Characterization of the sensor under the influence of analytes different ionic strengths is discussed in this section. Because the bio-analytical protocol should be performed in aqueous solution in the pH value range from 6 to 8, the ionic characterization of the sensor was investigated when applying of analyte solutions in different pH values, i.e., ionic strength, from 6 to 8. Note that the CNTs were not functionalized by the biotin in this characterization study. Real-time current response of the sensor was examined by respectively applying analyte solutions in pH values of 6.0, 7.0, and 8.0 on the sensing areas. The solutions were prepared based on the appropriate mixing of HCl and NaOH and adjusted by a benchtop pH meter (6175, Jenco Instruments, Inc.). The measurement was performed using an impedance analyzer (VerseSTAT 4, Princeton Applied Research) under ambient condition. Potential of 0.5 V was applied across the sensor and the current was measured continuously. The analyte solution was applied to the sensing area when the measurement started after 20 s. Real-time current response of the sensor is shown in Fig. 4(a). The current changed rapidly after the application of the solutions and became stable. The current change of the sensor was defined to be the difference between the current value before application of the analyte solution and the stable value after application. Hence, investigation of the current change in response to the pH value of the analyte solution was performed. The analyte solutions in different pH values, i.e., 6.0, 6.5, 7.0, 7.5, and 8.0, were prepared and respectively applied to the sensing areas. Quantitative correlation between the current change of the sensors and the pH value of the analyte solutions is shown in Fig. 4(b). The current change decreased with the increase of the pH values of the analyte solutions. Importantly, it was shown that the CNT-based sensor had stable electrical characteristic in the analyte solution with stable pH value. Typically, biological assays are conducted in aqueous solution in a stable pH value. Bio-molecules are suspended in buffer, e.g., PBS, to maintain a stable pH value for performing biological interaction. From our results, we can infer that the electrical output of the sensor showed stable when an analyte solution in a stable pH value is applied. This confirms the feasibility of the sensor for the application of biological assays.

The conductivity change of the CNT bundles is in response to the variations of the potential at the CNT's surface. When the OH group is introduced to the CNT's sidewall, a peak in the density of states (DOS) arises at the Fermi level (E_F) and the energy gap (E_{gap}) is significantly reduced [45]. This is because of the interaction between oxygen and carbon atom. OH group can form an acceptor level and enhance the conductivity of the CNT. Because the concentration of the OH group in the solution is represented by pH value, measurement of the resistance change of the CNT bundles can estimate the pH value of the analyte solution. Bundled CNT-based sensors fabricated on silicon substrate have been reported for the measurement of the pH value of the analyte solution [35]. The resistance of the CNT bundles across the microelectrodes showed proportional decrease to the pH value of the analyte solution. In our study, the pH response of the CNT-based sensor was also in reasonably agreement with the previous report.

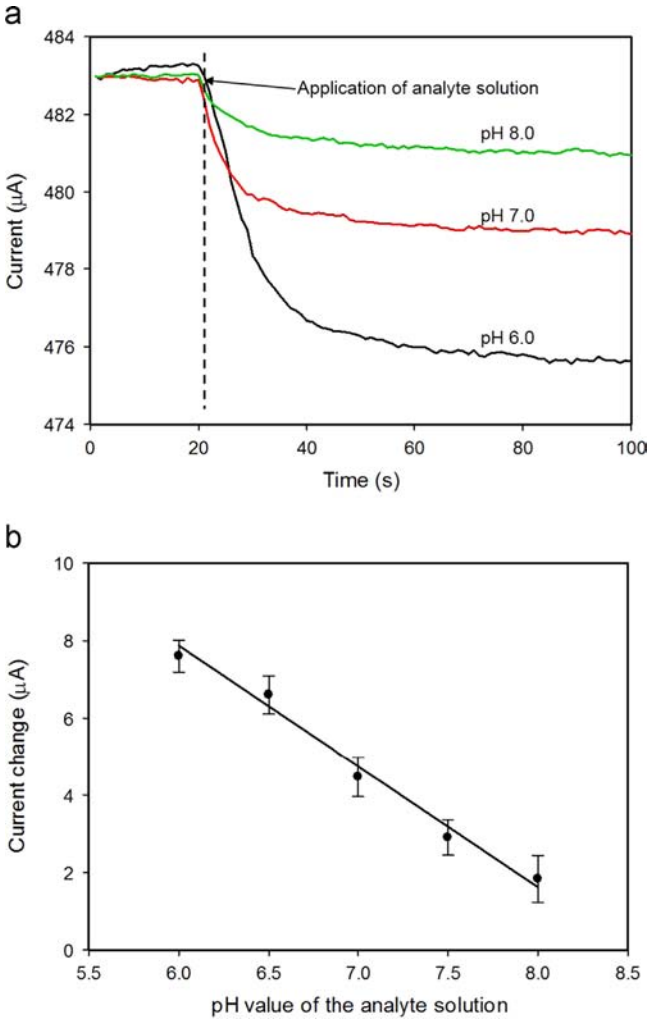

Fig. 4. Investigation of the chemical response of the CNT-based sensor. (a) Real-time current response of the sensors after respective applications of analyte solutions in different pH values of 6.0, 7.0, and 8.0. (b) Quantitative correlation between the current change of the sensor and the pH value of the analyte solution. A linear regression line is shown and error bars represent the standard errors of at least three repeated measurements.

3.3. Quantitative detection of label-free immunoassay

Quantitative detection of protein binding activity using CNTs was realized by the immobilization of biotin on CNT's sidewall. Protein binding, i.e., biotin and avidin binding, on CNT's sidewall can directly influence the conductivity of the CNTs. Biotin functionalized CNT was examined by transmission electron microscope (TEM). A representative TEM image of biotin functionalized CNTs is shown in Fig. 5. Biotin molecules decorated the CNT's sidewall for the biological transducer. Some of the amino groups of biotin were attached covalently to the carboxyl groups of the acid functionalized CNT's sidewall and other amino groups and carboxyl groups on biotin were free and capable of interaction with the avidin molecules. Since the conductivity of CNT is highly related to the protein binding on its sidewall, we have performed the electrical detection of biotin–avidin interaction using the CNT-based biosensor on paper, as illustrated in Scheme 1. Three-electrode measurement was performed using an impedance analyzer (VerseSTAT 4, Princeton Applied Research) under ambient condition. A constant potential was set to be 0.5 V and the current was measured. In the experiment, in order to wet the biosensor for the definition of the initial reference status, 75 μl PBS was applied to the sensing area. Another 75 μl avidin solution, i.e., avidin suspended in PBS, was then applied and the current response

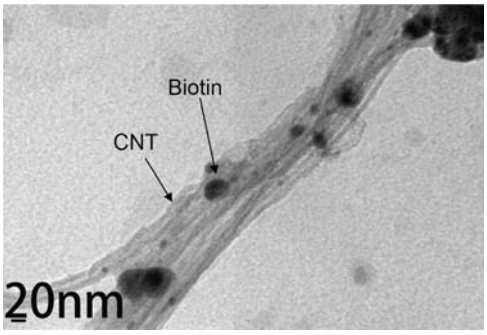

Fig. 5. TEM image of biotin functionalized CNTs.

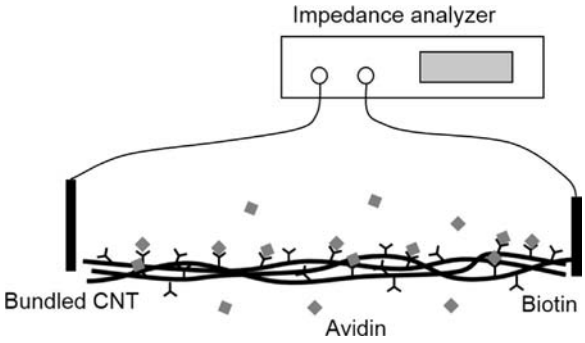

Scheme 1. Illustration of the electrical detection of biotin–avidin interaction using the CNT-based biosensor on paper.

was measured. Real-time current response of the biosensor after the respective applications of avidin solutions in different concentrations of 0 (control), 5, 50, and 500 ng/mL is shown in Fig. 6(a). Generally, higher concentration of the avidin solution induced larger decrease of the current. Avidin molecules interacted with the biotin molecules immobilized on the CNT's sidewall. It is clear that the presence of the target analyte, i.e., avidin in this case, reduced the current through the biosensor. The results agreed with the previous reports of biosensors using single CNT across the microelectrodes [30–33]. The decrease in conductance is due to the electron-donating property of the functional groups of protein [46]. Moreover, it was reported that at least 300 s is required for the formation of antibody–antigen complex [47]. In our results, real-time response showed that the starting time of the "flat" portion of the curve, i.e., steady-state response, was 500 s after the application of the target analyte. The transient response showed the progress of the biotin–avidin complex formation. Based on this observation, avidin solutions in different concentrations of 0 (control), 5, 25, 50, 250, and 500 ng/mL were prepared and respectively applied to the biosensors using the aforementioned procedures. Control was set to be the solution with 0 ng/mL avidin, i.e., only PBS. After the application of target analyte, at least 500 s was allowed to incubate in order to make sure that immune-reaction had enough time to proceed. The current change was measured and plotted in Fig. 6(b). It is generally expected that a fixed concentration of antigen is immobilized on a device, and the shifts in signal increased with increasing concentration of antibody in the solution [48]. The current change showed logarithmic proportionality to the concentration of avidin. The sensitivity was calculated to be 0.33 $\mu A/ng\,mL^{-1}$ and the minimal detectable analyte concentration was 25 ng/mL based on the analysis of statistical significance. In comparison to conventional immunoassay, detection of antibody–antigen binding relies on some labels to amplify the biological signal. Using a label can generate detectable signal; but, it induce extra operations and time cost. A conventional enzyme-linked immunosorbent assay (ELISA) requires well-trained

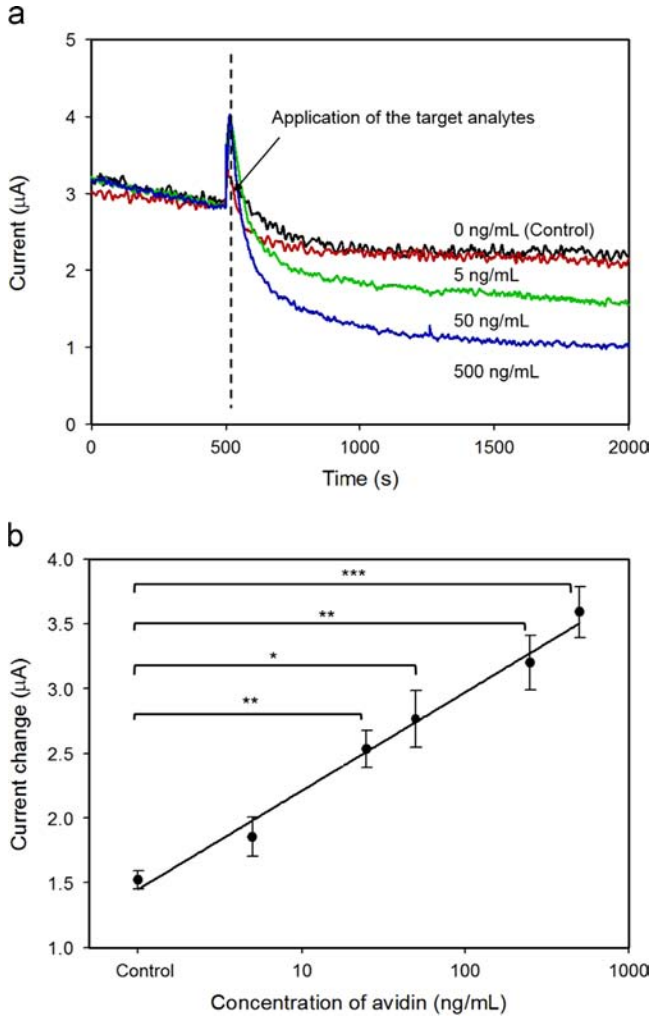

Fig. 6. Investigation of the electrical detection of label-free immunoassay using the CNT-based biosensor. (a) Real-time current response of the biosensors after respective applications of avidin solutions in different concentrations of 0 (control), 5, 50, and 500 ng/mL. (b) Quantitative correlation between the current change of the biosensor and the avidin concentrations of 0 (control), 5, 25, 50, 250, and 500 ng/mL. A linear regression line is shown and error bars represent the standard errors of at least three repeated measurements. Statistical significance was analyzed by one way analysis of variance (ANOVA) and indicated as $^{*}p < 0.01$, $^{**}p < 0.005$, and $^{***}p < 0.001$.

technician to operation and at least 6 h to complete. In this work, CNT was used as a semi-conducting electrode and its conductivity strongly depends on the presence of antibody–antigen complex on its sidewall. Label-free immunoassay could be achieved by single application of analyte (without the need of well-trained personnel) and requires 500 s, which is a large elimination of extra operations and time cost. These results indicated that the CNT-based biosensor developed in this study was capable to quantitatively perform the label-free immunoassay on paper-based microfluidic device.

4. Conclusion

To meet the requirement of rapid disease screening in clinics or home, a quantitative, portable, fast, simple to operate, and inexpensive immunoassay device has been developed. The CNT-based biosensor with well-controlled dimension was successfully fabricated on paper based on the proposed method. Because the conductivity of CNTs exhibits strong dependence on the presence of antibody–antigen complex on its sidewall, biotin was immobilized on CNTs to be used as a biological transducer. Implementation of a quantitative label-free immunoassay was demonstrated by direct measurement of the current change of the biosensor after single application of the target analyte, i.e., avidin. The time necessary for detection was 500 s which is a large reduction compared with conventional immunoassay. The proposed biosensor can be developed for a powerful device for POC applications. Importantly, this fabrication method is simple and efficient, and is a well-controlled technique to deposit CNT bundles for realizing a functional sensor on a paper-based microfluidic device.

Acknowledgment

Authors would like to thank the Chang Gung Memorial Hospital for the financial support (Project number: CMRPD2D0021).

References

[1] R.M. Lequin, Clin. Chem. 51 (2005) 2415–2418.
[2] P. Von Lode, Clin. Biochem. 38 (2005) 591–606.
[3] C.D. Chin, V. Linder, S.K. Sia, Lab Chip 7 (2007) 41–57.
[4] P. Yager, T. Edwards, E. Fu, K. Helton, K. Nelson, et al., Nature 442 (2006) 412–418.
[5] K.F. Lei, J. Lab. Autom. 17 (2012) 330–347.
[6] S.E. McCalla, A. Tripathi, Annu. Rev. Biomed. Eng. 13 (2011) 321–343.
[7] L. Wang, P.C.H. Li, Anal. Chim. Acta 687 (2011) 12–27.
[8] G.M. Whitesides, Nature 442 (2006) 368–373.
[9] A.W. Martinez, S.T. Philips, G.M. Whitesides, E. Carrilho, Anal. Chem. 82 (2010) 3–10.
[10] W. Dungchai, O. Challapakul, C.S. Henry, Anal. Chem. 81 (2009) 5821–5826.
[11] A.W. Martinez, S.T. Philips, B.J. Wiley, M. Gupta, G.W. Whitesides, Lab Chip 8 (2008) 2146–2150.
[12] E. Carrilho, A.W. Martinez, G.M. Whitesides, Anal. Chem. 81 (2009) 7091–7095.
[13] Y. Lu, W. Shi, L. Jiang, J. Qin, B. Lin, Electrophoresis 30 (2009) 1497–1500.
[14] D.A. Bruzewicz, M. Reches, G.M. Whitesides, Anal. Chem. 80 (2008) 3387–3392.
[15] X. Li, J. Tian, T. Nguyen, W. Shen, Anal. Chem. 80 (2006) 9131–9134.
[16] A.W. Martinez, S.T. Phillips, M.J. Butte, G.M. Whitesides, Angew. Chem. Int. Ed. 46 (2007) 1318–1320.
[17] A.W. Martinez, S.T. Phillips, E. Carrilho, S.W. Thomas III, H. Sindl, et al., Anal. Chem. 80 (2008) 3699–3707.
[18] A.K. Ellerbee, S.T. Phillips, A.C. Siegel, K.A. Mirica, A.W. Martinez, et al., Anal. Chem. 81 (2009) 8447–8452.
[19] Z. Nie, C.A. Nijhuis, J. Gong, X. Chen, A. Kumachev, et al., Lab Chip 10 (2010) 477–483.
[20] R.F. Carvalhal, M.S. Kfouri, M.H. de Ollverira Piazetta, A.L. Gobbi, L.T. Kubota, Anal. Chem. 82 (2010) 1162–1165.
[21] X. Ge, A.M. Asiri, D. Du, W. Wen, S. Wang, Y. Lin, Trends Anal. Chem. 58 (2014) 31–39.
[22] P. Zhou, Y.T. Lu, J. Zhu, J.B. Hong, B. Li, J. Zhou, D. Gong, A. Montoya, J. Agric. Food Chem. 52 (2004) 4355–4359.
[23] K. Glynou, P.C. Ioannou, T.K. Christopoulos, V. Syriopoulou, Anal. Chem. 75 (2003) 4155–4160.
[24] W.Y. Zhang, X.X. Ge, Y. Tang, D. Du, D.L. Liu, Y. Lin, Analyst 138 (2013) 5431–5436.
[25] G.D. Liu, Y.Y. Lin, J. Wang, H. Wu, C.M. Wai, Y. Lin, Anal. Chem. 79 (2007) 7644–7653.
[26] Y.F. Wu, P. Xue, Y.J. Kang, K.M. Hui, Anal. Chem. 85 (2013) 8661–8668.
[27] Y.F. Wu, P. Xue, K.M. Hui, Y.J. Kang, Biosens. Bioelectron. 52 (2014) 180–187.
[28] M. Wilchek, E.A. Bayer, Anal. Biochem. 171 (1998) 1–32.
[29] E.P. Diamandis, T.K. Christopoulos, Clin. Chem. 37 (1991) 625–636.
[30] A. Star, J.P. Gabriel, K. Bradley, G. Gruner, Nano Lett. 3 (2003) 459–463.
[31] C. Li, M. Curreli, H. Lin, B. Lei, F.N. Ishikawa, et al., J. Am. Chem. Soc. 127 (2005) 12484–12485.
[32] K. Maehashi, T. Katsura, K. Kerman, Y. Takamura, K. Matsumoto, et al., Anal. Chem. 79 (2007) 782–787.
[33] C. Lynam, N. Gilmartin, A.I. Minett, R. O'Kennedy, G. Wallace, Carbon 47 (2009) 2337–2343.
[34] C.K.M. Fung, V.T.S. Wong, R.H.M. Chan, W.J. Li, IEEE Trans. Nanotechnol. 3 (2004) 395–403.
[35] J.H. Kwon, K.S. Lee, Y.H. Lee, B.K. Ju, Electrochem. Solid-State Lett. 9 (2006) H85–H87.
[36] Z. Wu, Z. Chen, X. Du, J.M. Logan, J. Sippel, et al., Science 305 (2004) 1273–1276.
[37] D. Zhang, K. Ryu, X. Liu, E. Polikarpov, J. Ly, et al., Nano Lett. 6 (2006) 1880–1886.
[38] Y. Zhou, L. Hu, G. Gruner, Appl. Phys. Lett. 88 (2006) 123109.
[39] K.F. Lei, K.F. Lee, S.I. Yang, Microelectron. Eng. 100 (2012) 1–5.

[40] K.F. Lei, S.I. Yang, J. Nanosci. Nanotechnol. 13 (2013) 6917–6923.
[41] S. Bhattacharyya, C. Sinturel, J.P. Salvetat, M.L. Saboungi, Appl. Phys. Lett. 86 (2005) 113104.
[42] B.Q. Wei, R. Vajtai, P.M. Ajayan, Appl. Phys. Lett. 79 (2001) 1172–1174.
[43] F. Wakaya, K. Katayama, K. Gamo, Microelectron. Eng. 67–68 (2003) 853–857.
[44] J. Tersoff, Appl. Phys. Lett. 74 (1999) 2122–2124.
[45] H. Pan, Y.P. Feng, J.Y. Lin, Phys. Rev. B 70 (2004) 245425.
[46] K. Bradley, M. Brinman, A. Star, G. Guner, Nano Lett. 4 (2004) 253–256.
[47] L. Wang, W. Chen, D. Xu, B.S. Shim, Y. Zhu, et al., Nano Lett. 9 (2009) 4147–4152.
[48] Y. Sun, X. Liu, D. Song, Y. Tian, S. Bi, S. Zhang, Sens. Actuators B 122 (2007) 469–474.